JOURNAL OF AIRCRAFT
Vol. 31, No. 4, July–Aug. 1994

Lessons from Application of Equivalent Plate Structural Modeling to an HSCT Wing

Eli Livne*
University of Washington, Seattle, Washington 98195
and
Robert A. Sels† and Kumar G. Bhatia‡
Boeing Commercial Airplane Group, Seattle, Washington 98124

Equivalent plate wing models based on classical plate theory have been used for more than two decades as computationally efficient structural approximations for airplane preliminary design. Prior publications describing these models indicate satisfactory correlation with the corresponding finite element analysis and test results. In reality, a satisfactory correlation is not possible for certain types of structural wing concepts. The circumstances under which approximation by current wing equivalent plate theory is adequate are studied in this article. A Boeing HSCT wing model with low aspect ratio is used and correlations are shown for displacements, stresses, and natural frequencies and mode shapes. It is shown that current equivalent plate models based on classical plate theory are only adequate for wings with high transverse shear stiffness. Results based on a new equivalent plate formulation that accounts for transverse wing shear flexibility support this conclusion.

Introduction

Background

DETAILED finite element models, the standard tool used in airplane static and dynamic structural analysis, are computationally intensive. In addition, their generation, debugging, and verification can take a considerable amount of time even with advanced computer graphics and special pre- and postprocessors. In a preliminary design environment, where many configurations need to be studied before a final configuration is selected, the long time required to generate a new finite element model tends to slow down the design process and limit the number of configurations examined. In multidisciplinary optimization, where many analyses and sensitivity calculations are required during the automated search for an optimum design, structural analysis based on detailed finite element techniques can lead to long computation times even on current supercomputers.

The motivation for the development of approximate, "computationally cheap" structural models for preliminary design is thus twofold: 1) accelerate model preparation and analysis of new configurations, and 2) reduce computational cost of automated structural optimization and multidisciplinary optimization.

Beam models have been used for wing structural analysis from the early days of aviation. They are quite effective for the preliminary design of high aspect ratio, all metal wings. However, for composite materials and low aspect ratio wings, beam models can be totally inadequate. The sensitivity of composite beams to root boundary conditions and warping effects and the chordwise bending of low aspect ratio wings are some of the reasons for limitations of these models.[1,2]

Modeling low aspect ratio wings as equivalent plates, imposing Kirchhoff's kinematic assumptions of classical plate theory (CPT), and neglecting shear deformation in spar and rib webs was the approach to structural modeling adopted in the TSO aeroelastic wing optimization code.[3] In numerous applications and several correlation studies with experiment and finite element solutions, it has been shown that the TSO plate models can capture essential structural characteristics of realistic wings quite accurately.[3,4] Reasonable accuracy for the purpose of preliminary design in terms of static deformation and mode shapes (and the resulting static aeroelastic and flutter calculations) was demonstrated on the YF16 and F15 wings. Some applications to high aspect ratio wings in addition to more fighter type wings[5,6] have also been reported.

In Refs. 7 and 8 Giles reports modification and generalization of equivalent plate models based on classical plate theory for the modeling of cambered wings whose planform is made of several trapezoidal "boxes" (TSO can handle only one trapezoidal wing box and its control surfaces). Spar and rib caps are modeled directly in Refs. 7 and 8. Thus, the internal structure of the wing can be modeled and stresses are obtained in the skins as well as spar/rib caps. Giles' contribution, in addition to the capability to model multitrapezoidal wings, cambered wings, and spar/rib caps, extends to the numerical aspects of equivalent plate formulation. Rather than using well-behaved orthogonal polynomials for Ritz functions, as in TSO, he shows that good accuracy can be obtained with simple polynomials before stiffness and mass matrices become ill conditioned.[7] This leads to significant savings in CPU time since stiffness and mass matrix terms can be obtained by analytic integration. Giles' code (named ELAPS) has become well known and widely used by the aeronautic structural and multidisciplinary optimization community in recent years.

In an effort to improve efficiency even further and extend equivalent plate modeling to configurations that are needed in aeroservoelastic optimization, the lifting surface control augmented structural synthesis (LS-CLASS) code was developed at UCLA.[9,10] Like ELAPS, this code can handle configurations made of wings attached to a flexible, beam-like fuselage and to flexible control surfaces. In addition, all behavior sensitivities in LS-CLASS with respect to all sizing type and planform shape design variables are based on analytic

Received Feb. 21, 1993; presented as Paper 93-1413 at the AIAA/ASME/ASCE/AHS/ASC 34th Structures, Structural Dynamics, and Materials Conference, La Jolla, CA, April 19–21, 1993; revision received Sept. 12, 1993; accepted for publication Nov. 18, 1993.

*Assistant Professor, Aeronautics and Astronautics. Senior Member AIAA.
†Senior Engineer, HSCT Program.
‡Senior Principal Engineer, HSCT Program. Associate Fellow AIAA.

derivatives. Thus, the uncertainties and computational price typical of finite difference derivatives have been avoided.

Motivation

The Boeing HSCT wing presents a challenge to any equivalent plate modeling technique. It is cambered. It carries an array of leading-edge and trailing-edge control surfaces. Unlike the F15 and F16 wings, it has very few ribs. It is attached to a long and flexible fuselage and contains a major discontinuity in the form of a wheel bay area.

The potential benefits of multidisciplinary optimization in the preliminary design stage of the HSCT are well recognized. Following additional recent applications of the equivalent plate modeling approach,[11,12] a decision was made to pursue a similar approach at Boeing to evaluate the feasibility and benefits of this method, relative to traditional finite element practices, in a realistic preliminary design environment. Before embarking on an optimization effort using equivalent plates, it was decided to verify their accuracy and efficiency in the case of the HSCT wing by comparison to the corresponding finite element model using the airframe structural optimization code ELFINI.[13] The apparent lack of correlation between the results from the two representations led to a closer examination of the capabilities and limitations of classical equivalent plate models. It is believed the insights and lessons gained are unique and will provide an important experience base for users of equivalent plate models as well as directions for future research and development.

Scope of Article

This article opens with a description of the Boeing HSCT wing box models used. A systematic study of equivalent plate modeling limitations is described next. Alternative plate modeling practices are compared and discussed. Weaknesses and causes for inaccuracies are identified. Guidelines for the development of improved plate models are outlined, and results using these new plate models are described.

HSCT Wing Models

Topology and Geometry

The ELFINI finite element model of the HSCT wing box is shown in Fig. 1. The wing is attached to the fuselage along the side-of-body (SOB) rib and at the carry-through structure. It contains discontinuities in the form of a wheel bay and intersections of the SOB rib and carry-through structure, as well as the intersection of outer wing to inner wing. Control surfaces and engine nacelles are not considered at this stage. The wing contains an inboard section where chordwise deformation is extremely important as in typical low aspect ratio wings. The outboard wing, however, is of high aspect ratio structurally. It should be noticed that the wing contains many spars, but just a few ribs.

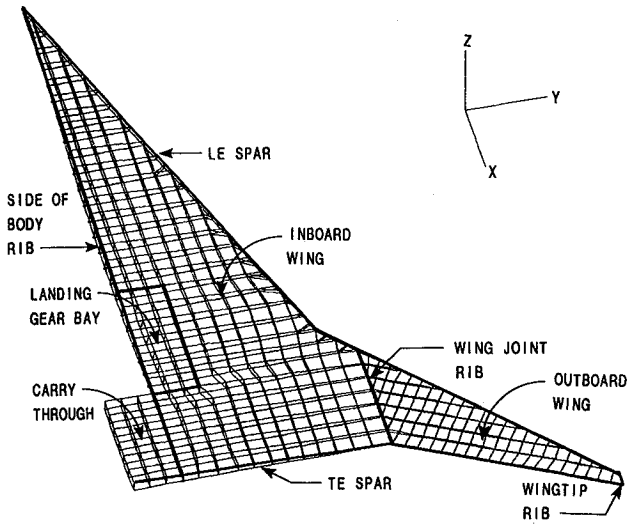

Fig. 1 ELFINI model of a Boeing HSCT wing box.

Three ELFINI wing box models are considered (Table 1 and Figs. 2 and 3): 1) a "simplified" model that has symmetry with respect to its middle plane, has no wheel bay, and its depth varies linearly from root to tip; 2) a "cambered" wing model that includes camber and depth distributions of the HSCT wing studied but no wheel bay; and 3) a third model, an "actual" HSCT wing model includes the wheel bay area as well as camber and depth distributions of the studied wing. This hierarchy in modeling complexity is required in order to study separately the effects of camber and discontinuities due to the wheel bay. The corresponding equivalent plate models are all symmetric (contain no camber). Polynomial series are used to define depth distribution of the plate models and were obtained by least squares fitting of the finite element nodal data. Figures 2 and 3 show geometric contour lines of the actual HSCT wing and its corresponding equivalent plate model in the spanwise direction and along several chordwise cuts. Depth distributions for the simplified wing are also shown in Figs. 2 and 3. In this case, the finite element and the corresponding plate models have identical depth distributions.

Table 1 Wing models evaluated numerically

	Camber	Depth	Wheel bay
HSCT wing (actual)	HSCT (—·—)[a]	HSCT (—·—)[a]	Yes
Simplified cambered	HSCT (—·—)[a]	HSCT (—·—)[a]	No
Simplified symmetric	No (---)[a]	Linear root to tip (---)[a]	No

Note: in the plate modeling of the actual HSCT wing, only polynomial depth is taken into account. No camber is included in the plate model, whereas the ELFINI model includes camber.
[a]Figs. 2 and 3.

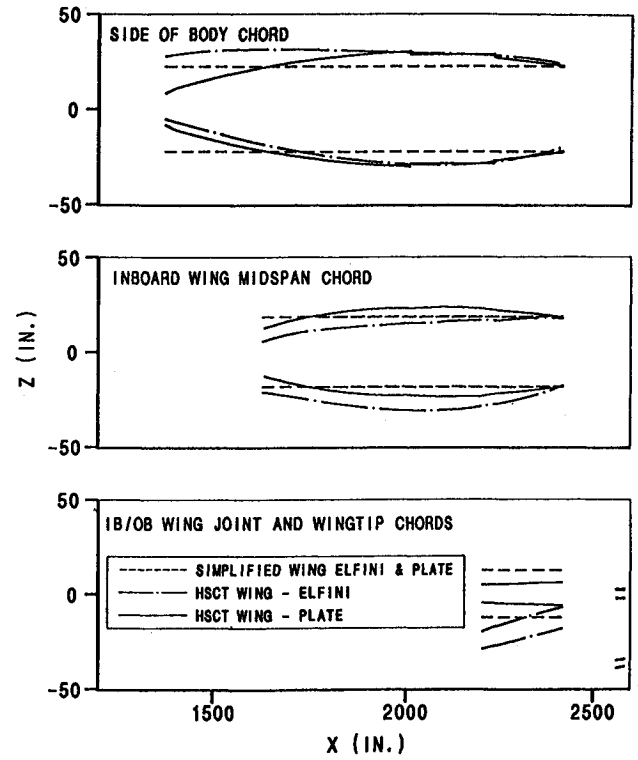

Fig. 2 Comparison of wing depth for the actual HSCT wing: ELFINI and LS-CLASS models (spanwise).

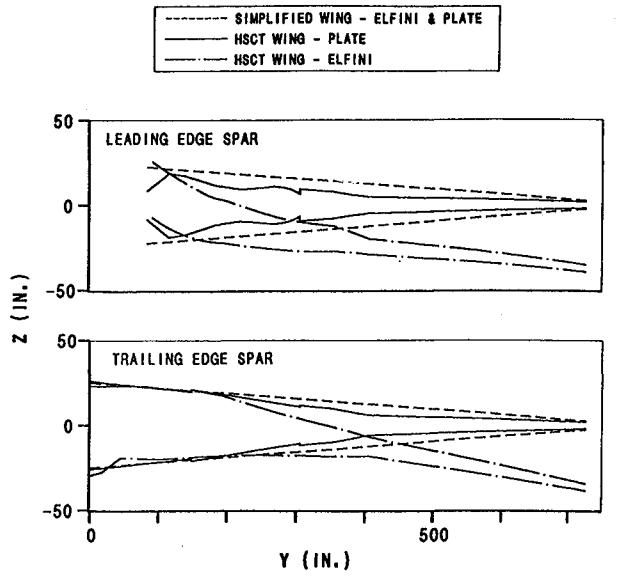

Fig. 3 Comparison of wing depth for the actual HSCT wing: ELFINI and LS-CLASS models (chordwise).

Sizing and Material Properties

The wing skins are made of composite material layers with the following on axis material properties:

E_{11} = 249.633 GPa (0.362×10^8 psi)
E_{22} = 9.654 GPa (0.14×10^7 psi)
ν_{12} = 0.29
G_{12} = 4.593 GPa (0.666×10^6 psi)
specific gravity = 1.58

Four fiber directions (0, 90, 45, and −45 deg with respect to spar direction) are used in the inboard wing. Four fiber directions (0, 90, 45, −45 deg with respect to the outboard wing spar lines) are used on the outboard wing. The thickness of a single ply is 0.09398 mm (0.0037 in.), and there are 20 plies in each fiber direction (representing a sandwich skin with 10 plies in each fiber direction on each face). Spar and rib caps are made of composite material with the following uniaxial properties:

E = 96.543 GPa (0.14×10^8 psi)
ν = 0.46

and the same specific gravity as the skins. Spar and rib webs are made of the same material as the skins. Four ply directions are used (0, 45, −45, and 90 deg).

Details of ELFINI and LS-CLASS Modeling Practices

The finite element model is made of membrane (plane stress) elements for skins, and a combination of shear and rod (truss) elements for spars and ribs. An exception is the case of the wing with a cutout for the landing gear, in which the skin over the wheel bay was modeled using bending plate elements. A single static load of a uniform 1 psi pressure over the wing planform is used for static deflection and stress calculations. Mode shapes and natural frequencies are calculated with the theoretical structural mass matrix.

The LS-CLASS equivalent plate model is divided into four "zones" (also denoted "global systems" in Ref. 9). Zone II is divided into four trapezoidal segments and each of the other three zones has a single trapezoidal segment associated with it. The relation between zones and trapezoidal segments is detailed below. In each zone a separate polynomial Ritz series is used to approximate the vertical displacement of the wing. Thus, over the first zone

$$w_1(x, y) = \{1, x, y, x^2, xy, y^2, x^3, \ldots\} \begin{Bmatrix} q_1^1 \\ q_2^1 \\ q_3^1 \\ \cdot \\ \cdot \\ \cdot \end{Bmatrix}$$

$$= \{1, x, y, x^2, xy, y^2, x^3, \ldots\}\{q^1\}$$

and over the second zone

$$w_2(x, y) = \{1, x, y, x^2, xy, y^2, x^3, \ldots\} \begin{Bmatrix} q_1^2 \\ q_2^2 \\ q_3^2 \\ \cdot \\ \cdot \\ \cdot \end{Bmatrix}$$

$$= \{1, x, y, x^2, xy, y^2, x^3, \ldots\}\{q^2\}$$

Compatibility of slope and deflection between the two zones is imposed by a series of very stiff springs at the outer/inner wing interface.

Each zone can be subdivided into trapezoidal elements that are used in the area integrations needed for stiffness and mass matrix elements.[9] Zones are therefore used as large elements in a p-type finite element method with compatibility imposed by a penalty function approach[14] using stiff springs. The equivalent plate modeling technique described so far is based on the kinematic assumptions of CPT, and does not account for transverse shear deformation, and in particular, the contribution of the spar and rib webs.

The continuous behavior of simple polynomial functions used in the original equivalent plate modeling techniques tends to smooth out any local effects due to geometric discontinuities. Breaking a wing configuration into several zones makes it possible to capture structural behavior in a piecewise continuous manner. It also makes it possible to use lower-order polynomials in the displacement series, thus preventing the numerical ill conditioning reported in Refs. 7–9. Results reflecting alternative selection of zones in modeling the wing will be studied and discussed in this article.

All major spars and ribs are included in the LS-CLASS model and are represented by their caps. Several short spars, whose effect is local, were neglected. This, in addition to the lack of spar/rib web modeling in the equivalent plate approach, leads to a small difference between the predicted theoretical weights of the ELFINI and LS-CLASS models.

Boundary Conditions and Load Case

Boundary conditions in LS-CLASS are imposed in two ways. For a simple configuration with a straight root, the Ritz polynomial functions can be selected to ensure zero displacement and slope along that root. Alternatively, the boundary conditions can be imposed by attaching the wing to the ground via a set of stiff linear and rotational springs. When the stiffness of these root springs is very high compared with wing stiffness they practically cantilever the wing by enforcing zero displacements and zero slopes.

Root springs offer an advantage, however, in that they can be used to simulate local flexibilities that cannot be captured by the equivalent plate model. Thus, in fine tuning the structural model to match the results of experiments, root springs can take into account the local flexibility of the support since no experimental setup guarantees ideal rigid support (Ref. 15, pp. 90–93).

Two sets of boundary conditions are used for this study. The wing is cantilevered in the first case (case A). This case

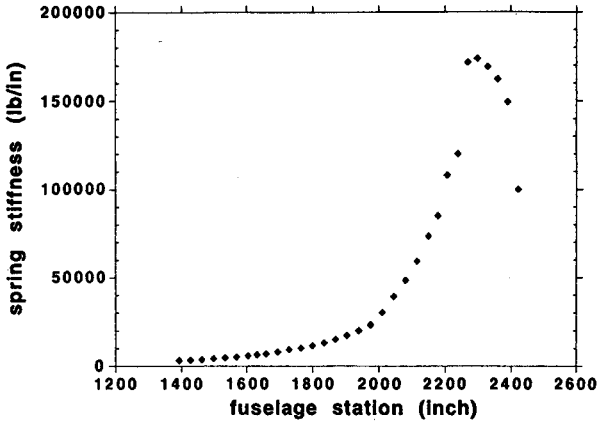

Fig. 4 Distribution of linear springs representing fuselage vertical flexibility.

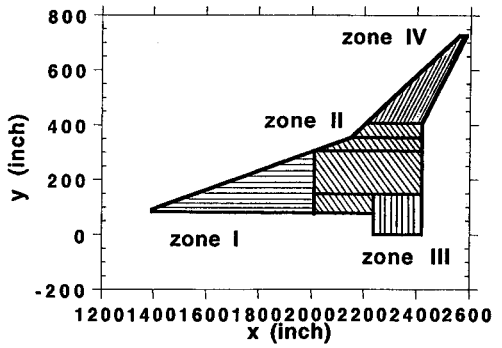

Fig. 5 The LS-CLASS CPT plate model (division into area trapezoids and zones).

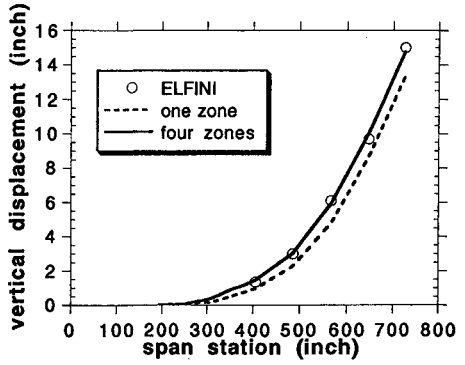

Fig. 6 Leading-edge deformation of the cantilevered wing under 1-psi uniform pressure load (actual HSCT wing).

is used for studying aspects of equivalent plate modeling such as the effect of the number of zones used and different representations of the wheel bay area. In the more interesting case of boundary conditions (case B), the wing is attached to the ground through a series of vertical linear springs representing fuselage flexibility (Fig. 4). The effect of fuselage-wing interaction can thus be studied. As will be shown, this interaction is extremely important in the case of the HSCT as compared with typical fighter wings that are usually attached to a relatively stiff and short fuselage.

A 1-psi uniform load over the wing is the static load case considered.

Aspects of Equivalent Plate Modeling

Different models were compared in the case of the cantilevered wing in order to study the following aspects of equivalent plate modeling based on classical plate theory: 1) the order of displacement polynomials needed, 2) alternative zone

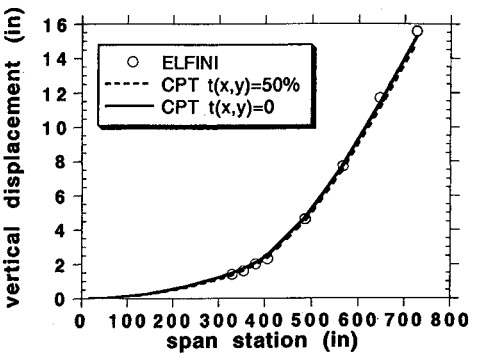

Fig. 7 Effect of wheel bay skin thickness representation on trailing-edge displacements of the CPT model (actual HSCT wing).

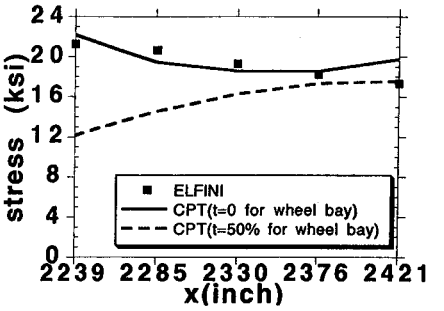

Fig. 8 Effect of wheel bay thickness representation in the CPT model on stresses at span station y = 111 in. (lower skin, σ_{11} for the 0-deg layer, actual HSCT wing).

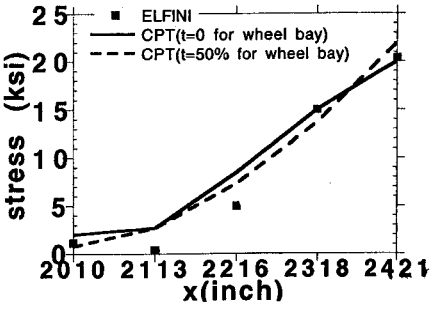

Fig. 9 Effect of wheel bay thickness representation in the CPT model on stresses at span station y = 305.1 in. (lower skin, σ_{11} for the 0-deg layer, actual HSCT wing).

models, and 3) the effect of the wheel bay opening on stresses and displacements.

Examination of different orders of Ritz polynomials and zonal arrangements led to a 4-zone model based on seventh-order Ritz polynomials in each of the zones. The breakup of the wing into four zones was guided by the presence of the wheel bay cutout in the wing and the stress concentration it produces (Figs. 1 and 5). Deformation along the leading edge obtained with one and four zones are compared to the ELFINI result in Fig. 6 for the cantilevered case. Rotational springs of 2.5×10^{10} lb-in./rad are used at the root to compensate for local differences in modeling between the finite element and plate models. With four zones, the correlation is excellent.

The wheel bay area presents a difficulty to the plate modeling. Since the LS-CLASS plate model assumes symmetry about midplane, it cannot handle directly a case in which there is an upper skin and no lower skin. Equivalent plate trailing-edge deformation based on zero skin thickness and half the actual thickness of the wing skin is shown in Fig. 7. The effect of the wheel bay on structural deformation is found to be very small in the case of the cantilevered wing. The effect of the wheel bay on lower skin stresses is examined in Figs. 8

and 9. As we move away (outboard) from the wheel bay, its effect on equivalent plate stresses diminishes. On the outboard wing, plate stresses obtained assuming 0 thickness or 10-ply thickness for the wheel bay skin are practically identical.

As can be seen, the correlation between the finite element and equivalent plate models for the cantilevered wing is reasonable in the static case in spite of the differences in transverse shear stiffness. The effect of transverse shear is discussed in the next section.

ELFINI/Equivalent Plate Correlation for the Wing on Springs Representing Fuselage Flexibility

Once the equivalent plate model was established for the wing, it was used for extensive comparisons with the different ELFINI finite element models. Case B boundary conditions were selected because of the anticipation of strong coupling between fuselage and wing stiffnesses and the importance of chordwise bending in the inboard wing. Initial equivalent plate results compared quite poorly with the ELFINI results for both stresses and static displacements, as well as mode shapes and frequencies. The plate model was found to be too stiff. This was especially apparent in the chordwise direction.

In an effort to better understand the reason for this behavior, the simplified wing model was used. Thus, differences between the ELFINI and plate models due to camber or wheel bay were not present. A comparison of chordwise displacements of the ELFINI simplified model and the equivalent plate model is shown in Fig. 10. The plate model cannot capture the chordwise bending along the side-of-body rib and in the inboard wing area properly.

The reported success of equivalent plate models for the F16 and F15 wings (Refs. 3 and 4) suggested one reason for the differences between ELFINI and LS-CLASS in the case of the HSCT wing box. The F16 and F15 wings are densely packed in terms of internal structure and include multiple strong ribs to support external store carriage points. The HSCT wing used for the present study contains only three full chord ribs as shown in Fig. 1. The lack of strong ribs will explain the differences in deformations along the SOB rib as shown in Fig. 10. The plate model, based on Kirchoff's hypothesis,[16] is inherently stiffer chordwise and cannot portray such chordwise behavior.

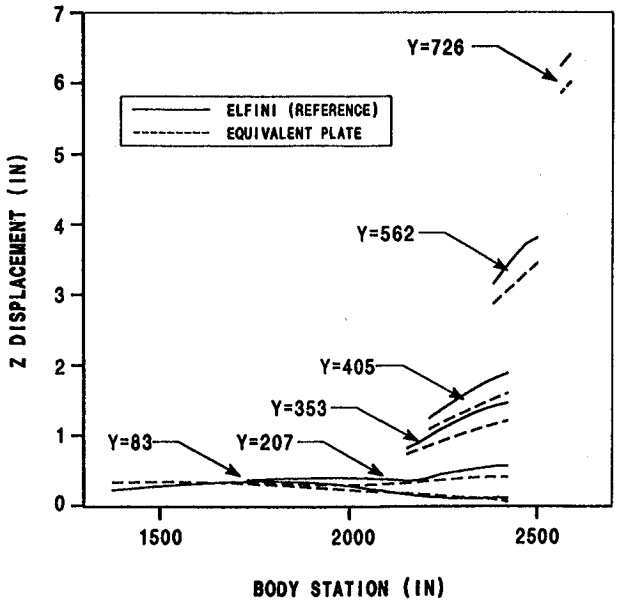

Fig. 10 Elastic deformation predicted by the ELFINI model and the equivalent plate CPT model (simplified wing).

Further support of this hypothesis comes from Ref. 7. The finite element model used to test the ELAPS model in Ref. 7 contains two trapezoidal elements, each containing 10 ribs and 11 spars represented by thick webs. It is, thus, a finite element model well described by a CPT plate model.

To prove this hypothesis, ribs were added to the ELFINI model of the simplified wing along all possible rib lines provided by the finite element mesh shown in Fig. 1. Elastic deformations for this model are compared (Fig. 11) with equivalent plate results. The correlation is somewhat improved, but the plate model is still too stiff. As a next step, the effect of shear stiffness due to rib and spar webs was examined. Figure 12 shows elastic deformation comparisons between plate results and ELFINI results based on added web shear stiffness in both spars and ribs. The web shear stiffness increase is by a factor of about 6 compared to the baseline design. Good correlation is obtained between equivalent plate

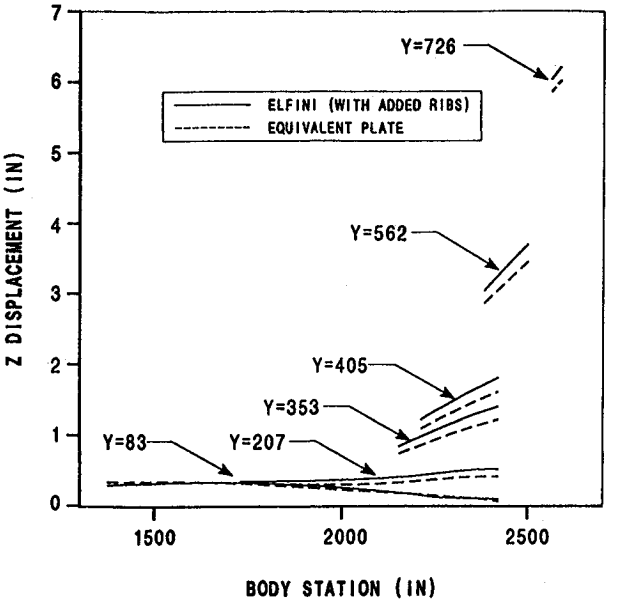

Fig. 11 Elastic deformation predicted by the ELFINI model with added ribs and the equivalent plate CPT model (simplified wing).

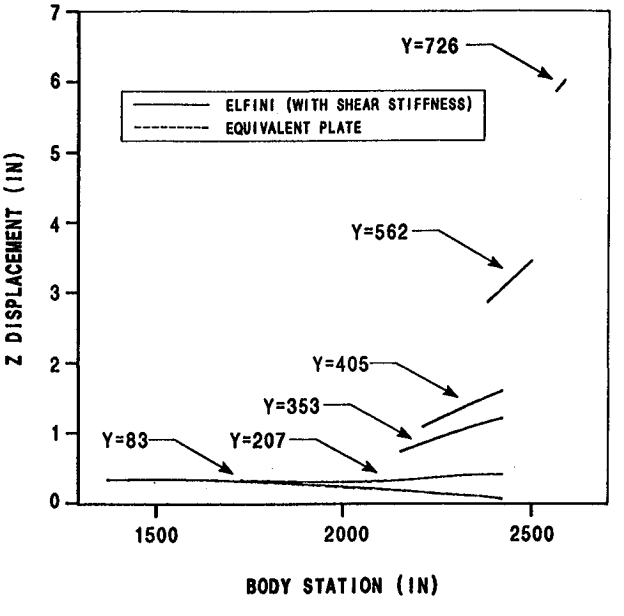

Fig. 12 Elastic deformation predicted by the ELFINI model with added ribs (including increased rib and spar web stiffness) and the equivalent plate CPT model (simplified wing).

and finite element results when the finite element model contains multiple spars and multiple ribs with high web shear stiffness. Improved correlation for stresses and mode shapes is also obtained when the finite element model has been stiffened in transverse shear (Figs. 13–15 and Table 2).

To further identify possible sources for disagreement between LS-CLASS and ELFINI results for the actual HSCT wing, an HSCT wing was modified by adding ribs (wherever possible according to the finite element mesh) and thickening the spar and rib webs. The ELFINI model has the camber and twist distributions of the wing, whereas the corresponding plate model is symmetric with respect to the midwing surface

Table 2 Natural frequencies with root springs for the simplified HSCT wing stiffened by the addition of ribs and increased shear web thickness

Mode	ELFINI (stiffened), Hz	LS-CLASS, Hz
1	9.9	9.90
2	26.6	26.2
3	28.0	28.1
4	36.6	39.3
5	39.6	56.6

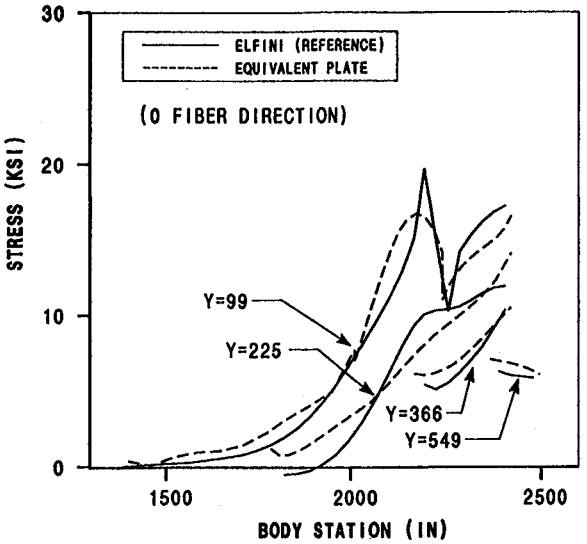

Fig. 13 Stresses predicted by the ELFINI model and the equivalent plate CPT model (0-deg fiber along fiber direction, simplified wing).

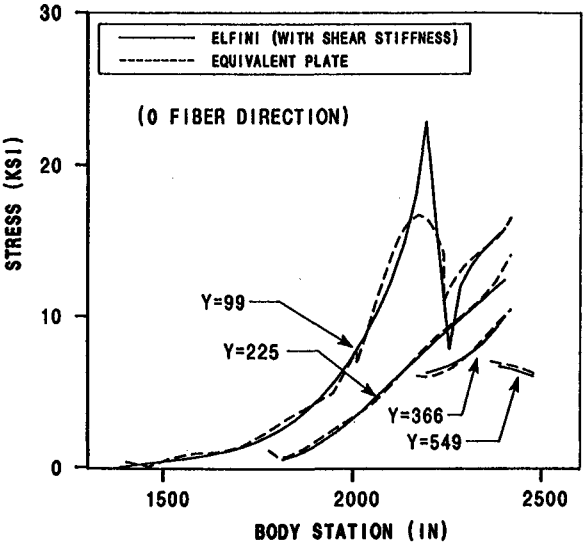

Fig. 14 Stresses predicted by the ELFINI model with added ribs (including increased rib and spar web stiffness), and the equivalent plate CPT model (along fiber direction, 0-deg fiber, simplified wing).

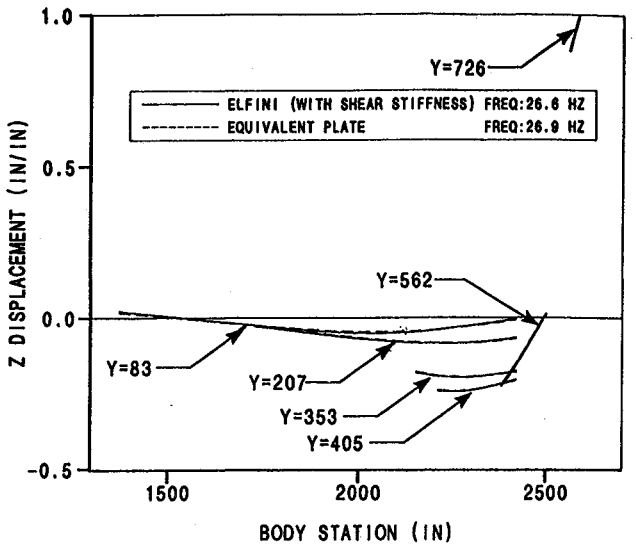

Fig. 15 Second mode shape—CPT equivalent plate and ELFINI model with added ribs and increased rib/spar web shear stiffness (simplified wing).

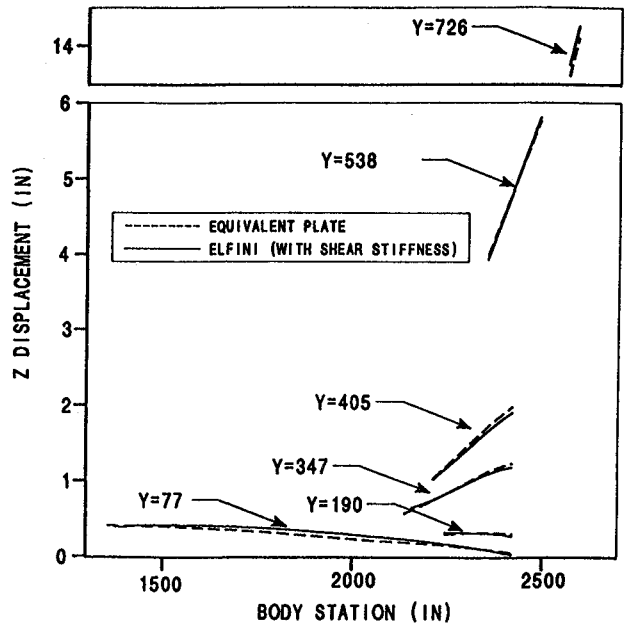

Fig. 16 Displacements of the actual HSCT wing with increased transverse stiffness including camber and twist effects.

(Table 1 and Figs. 2 and 3). The effect of camber on the accuracy of equivalent plate results has already been discussed in Ref. 8 and studied using a model of a fighter-type wing. Effects of twist and camber in the case of the HSCT wing are shown in Figs. 16 and 17, which contain displacement and stress correlations. The comparisons are good with differences in stress distribution near areas of stress concentration due to geometric discontinuities. It should be noticed that the division of the wing to four zones (Fig. 5) in the plate model makes it possible to capture the stress discontinuity that would otherwise be averaged and smeared if only one zone was used for the whole wing.

It is evident then that discrepencies in results between the plate and ELFINI models in the case of the HSCT wing are due to the inability of the CPT to represent the small number of ribs and the thin spar and rib webs. Thus, transverse shear representation and effects of the internal structure are the main causes of differences between classical equivalent plate and finite element results for the Boeing HSCT wing used in the present study.

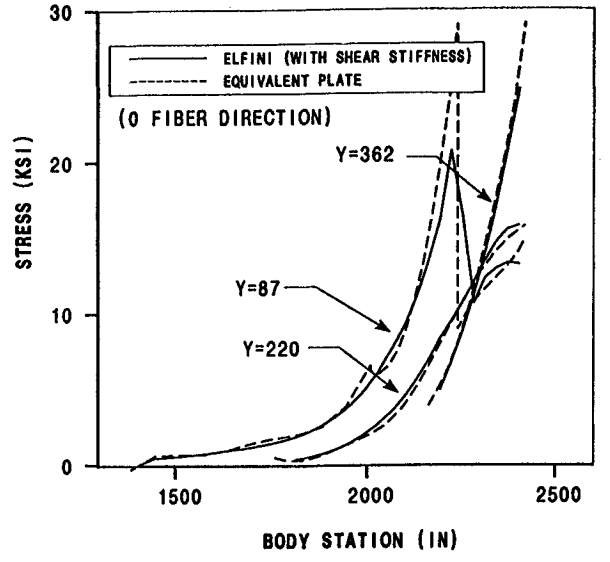

Fig. 17 Stresses in the actual HSCT wing with increased transverse stiffness including camber and twist effects (σ_{11} for the 0-deg layer).

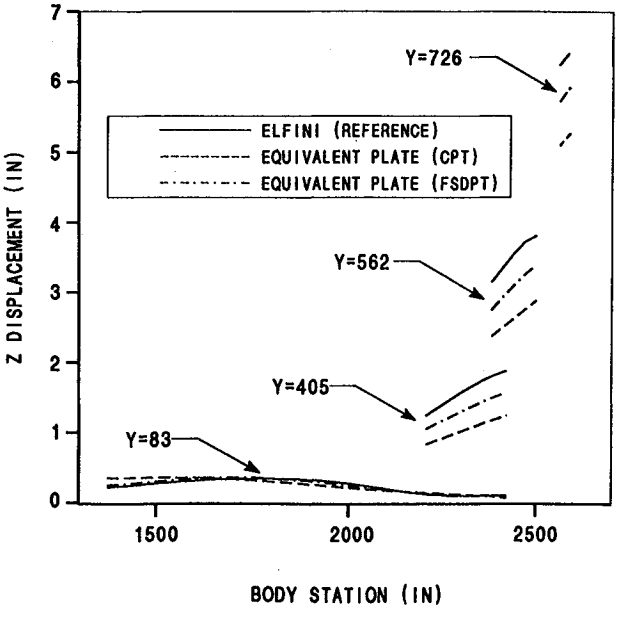

Fig. 18 Comparison of displacements of the simplified HSCT wing (with actual shear stiffness) evaluated by ELFINI and by CPT and FSDPT equivalent plates with stiff root springs.

New Equivalent Plate Modeling Technique Including Transverse Shear

The findings described in the previous sections motivated the development of a new equivalent plate wing modeling capability. It is based on the kinematic assumptions of first-order shear deformation plate theory (FSDPT),[16] and is described in detail in Ref. 17. The new capability includes modeling of the spar and shear webs directly, including details of their construction such as fiber directions and the number of layers in each fiber direction. Therefore, spar and rib webs are treated in a similar manner to the skin covers. Simple polynomials are used for Ritz functions and for depth and thickness distributions. Analytic formulas were obtained for the contribution of each spar, rib, and wing skin panel to the stiffness and mass matrices. This leads not only to computational efficiency (no numerical integration is needed), but also to closed form analytical expressions for the derivatives

Table 3 Natural frequencies of the simplified wing (actual ribs and spars) supported by springs representing fuselage stiffness along SOB rib (y = 83 in.)

ELFINI, Hz	FSDPT, Hz (% error)	CPT, Hz (% error)
9.5	9.2 (3%)	10.1 (6%)
23.9	23.4 (2%)	27.2 (14%)
26.9	24.7 (8%)	28.2 (5%)
33.7	30.3 (10%)	39.8 (18%)
36.1	32.5 (10%)	47.2 (31%)
42.7	43.6 (2%)	53.7 (26%)
45.2	49.0 (8%)	56.9 (26%)
49.6	50.5 (2%)	68.0 (37%)

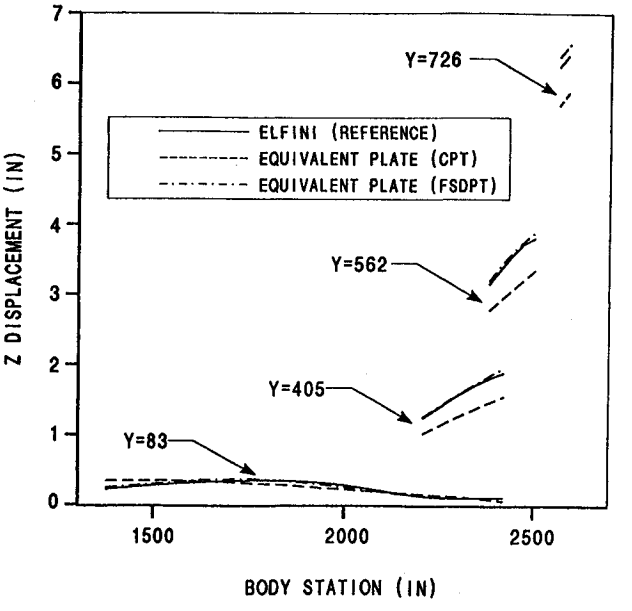

Fig. 19 Comparison of displacements of the simplified HSCT wing (with actual shear stiffness) evaluated by ELFINI and by CPT and FSDPT equivalent plates with soft root springs.

of stiffness and mass matrices with respect to sizing and shape design variables for the wing. Alternatively, in an effort to save computational time in a case with many spars and ribs, the array of spar and rib webs can be modeled as an equivalent core of a sandwich construction. Integration for stiffness and mass matrix contributions is done in this case for one core per area trapezoid, and not repeatedly for each spar and rib web.

Displacement comparisons for the simplified HSCT wing supported along the SOB rib by vertical springs representing fuselage flexibility (boundary conditions case B) including results from ELFINI, LS-CLASS(CPT), and the new FSDPT wing plate model are shown in Figs. 18 and 19. In the results of Fig. 18, both plate models included very stiff rotational springs (1.0×10^{14} lb-in./rad) along the SOB rib and center line to enforce a zero spanwise slope exactly. The advantage of the new plate model (including transverse shear stiffness) over the classical plate theory model is clear. Rotational springs of 2.5×10^{10} lb-in./rad along the SOB rib and centerline in the CPT model, and the corresponding y-direction springs on the upper and lower skins along the SOB rib and centerline in the FSDPT model lead to the results in Fig. 19. This compensation for the local deformation of the finite element model along the lines of support, improves correlation with the two alternative plate models. A list of natural frequencies in Table 3 provides another demonstration of the importance of transverse shear in the present case.

Summary and Conclusions

Equivalent plate modeling practices were discussed in the context of application to a Boeing HSCT wing. For models based on CPT, effects of using zones and effects of a wheel bay discontinuity were examined. Extensive studies of equivalent plate modeling revealed limitations of the CPT models. These models are consistently stiffer than the corresponding finite element models and portray strong coupling between bending and torsional behavior. The plate models as used today in TSO,[2] ELAPS,[7,8] and LS-CLASS[9,10] seem to be adequate only in the case of low aspect ratio wings with many spars and ribs and high transverse shear stiffness. The equivalent plate models are inadequate for an HSCT wing because the wing does not have a high transverse shear stiffness. This inadequacy was more evident when the fuselage flexibility effects were accounted for in the boundary conditions. A newly developed equivalent plate wing modeling capability based on first-order shear deformation plate theory (FSDPT) leads to better correlation with finite element results for the HSCT wing and shows promise as a fast, effective structural analysis and behavior sensitivity tool for preliminary design.

Acknowledgments

The authors would like to thank Gary Giles of NASA Langley Research Center for many helpful discussions. Verification of the LS-CLASS results by corresponding selected ELAPS test cases helped direct this research to focus on limitations inherent to the CPT wing modeling. The insight and experience of Jiri Wertheimer from the Boeing Company contributed to this work, and his support is warmly acknowledged.

References

[1]Lottati, I., "Flutter and Divergence Aeroelastic Characteristics for Composite Forward Swept Cantilevered Wing," *Journal of Aircraft*, Vol. 22, No. 11, 1985, pp. 1001–1007.

[2]Librescu, L., and Simovich, J., "A General Formulation for the Aeroelastic Divergence of Composite Swept Forward Wing Structures," *Journal of Aircraft*, Vol. 25, No. 4, 1988, pp. 364–371.

[3]Lynch, R. W., Rogers, W. A., and Brayman, W. W., "Aeroelastic Tailoring of Advanced Composite Structures for Military Aircraft," U.S. Air Force Flight Dynamics Lab. Rept. AFFDL-TR-76-100, April 1977.

[4]Triplett, W. E., "Aeroelastic Tailoring Studies in Fighter Aircraft Design," *Journal of Aircraft*, Vol. 17, No. 7, 1980, pp. 508–513.

[5]Schweger, J., Sensburg, O., and Berns, H., "Aeroelastic Problems and Structural Design of a Tailless CFC Sailplane," 2nd International Symposium on Aeroelasticity and Structural Dynamics, Aachen, Germany, April 1985.

[6]Sensburg, O., Schmidinger, G., and Fullhas, K., "Integrated Design of Structures," *Journal of Aircraft*, Vol. 26, No. 3, 1989, pp. 260–270.

[7]Giles, G. L., "Equivalent Plate Analysis of Aircraft Wing Box Structures with General Planform Geometry," *Journal of Aircraft*, Vol. 23, No. 11, 1986, pp. 859–864.

[8]Giles, G. L., "Further Generalization of an Equivalent Plate Representation for Aircraft Structural Analysis," *Journal of Aircraft*, Vol. 26, No. 1, 1989, pp. 67–74.

[9]Livne, E., Schmit, L. A., and Friedmann, P. P., "Design Oriented Structural Analysis for Fiber Composite Wings," Dept. of Mechanical, Aerospace and Nuclear Engineering, Univ. of California, UCLA Rept. UCLA-ENG-88-36, Los Angeles, CA, Nov. 1988.

[10]Livne, E., "Integrated Multidisciplinary Optimization of Actively Controlled Fiber Composite Wings," Ph.D. Dissertation, Mechanical, Aerospace and Nuclear Engineering Dept., Univ. of California, Los Angeles, CA, 1990.

[11]Barthelemy, J-F. M., Coen, P. G., Wrenn, G. A., Riley, M. F., Dovi, A. R., and Hall, L. E., "Application of Multidisciplinary Optimization Methods to the Design of a Supersonic Transport," NASA TM-104073, March 1991.

[12]Chang, K. J., Haftka, R. T., Giles, G. L., and Kao, P. J., "Sensitivity Based Scaling for Correlating Structural Response from Different Analytical Models," AIAA Paper 91-0925, April 1991.

[13]Lecina, G., and Petiau, C., "Advances in Optimal Design with Composite Materials," *Computer Aided Optimal Design: Structural and Mechanical Systems*, edited by C. A. Mota Soares, Springer-Verlag, 1987.

[14]Kao, P. J., "Coupled Rayleigh-Ritz/Finite Element Structural Analysis Using Penalty Function Method," *AIAA/ASME/ASCE/AHS/ASC 33rd Structures, Structural Dynamics and Materials Conference* (Dallas, TX), AIAA, Washington, DC, 1992, Pt. I, pp. 135–141 (AIAA Paper 92-2238).

[15]Gallagher, R. H., Rattinger, I., and Archer, J. S., "A Correlation Study of Methods of Matrix Structural Analysis," Macmillan, New York, 1964 (AGARDograph 69).

[16]Reddy, J. N., "Energy and Variational Methods in Applied Mechanics," Wiley, New York, 1984, Chap. 4.

[17]Livne, E., "Recent Developments in Equivalent Plate Wing Modeling for Shape Optimization," AIAA Paper 93-1647, April 1993.